

# Nanoscale

Accepted Manuscript



This is an *Accepted Manuscript*, which has been through the Royal Society of Chemistry peer review process and has been accepted for publication.

*Accepted Manuscripts* are published online shortly after acceptance, before technical editing, formatting and proof reading. Using this free service, authors can make their results available to the community, in citable form, before we publish the edited article. We will replace this *Accepted Manuscript* with the edited and formatted *Advance Article* as soon as it is available.

You can find more information about *Accepted Manuscripts* in the [Information for Authors](#).

Please note that technical editing may introduce minor changes to the text and/or graphics, which may alter content. The journal's standard [Terms & Conditions](#) and the [Ethical guidelines](#) still apply. In no event shall the Royal Society of Chemistry be held responsible for any errors or omissions in this *Accepted Manuscript* or any consequences arising from the use of any information it contains.

# Conductivity scaling in supercritical percolation of nanoparticles

## – Not a power law

Jiantong Li\* and Mikael Östling

*KTH Royal Institute of Technology, School of Information and Communication Technology,*

*Electrum 229, 16440 Kista, Sweden*

\*E-mail: [jiantong@kth.se](mailto:jiantong@kth.se)

The power-law behavior widely observed in supercritical percolation systems of conductive nanoparticles may merely be a phenomenological approximation to the true scaling law not yet discovered. In this work, we derive a comprehensive yet simple scaling law and verify its extensive applicability to various experimental and numerical systems. In contrast to the power law which lacks theoretical backing, the new scaling law is explanatory and predictive, and thereby helpful to gain more new insights into percolation systems of conductive nanoparticles.

Conductive nanoparticles (CNPs), such as one-dimensional (1D) carbon nanotubes and metal nanowires,<sup>1-5</sup> two-dimensional (2D) graphene and MoS<sub>2</sub> nanosheets,<sup>6-8</sup> and three-dimensional (3D) spherical metal particles,<sup>9</sup> are attractive materials for emerging electronics and advanced energy storage and conversion.<sup>9-13</sup> The knowledge of conductivity scaling in composites (or percolation systems) comprising CNPs is crucially important for many applications. At present, the overwhelming majority of studies<sup>5,9,14-17</sup> employ a power law to describe the conductivity  $\sigma$  of a CNP percolation system in the form as

$$\sigma = \sigma_0(\phi - \phi_0)^s, \quad (1)$$

where  $\sigma_0$  is a pre-exponential factor,  $\phi$  can be any observable equivalent to the volume fraction, and  $\phi_0$  and  $s$  are, more often than not, *assumed* as the percolation threshold and critical conductivity exponent, respectively. In experiments, the power law often applies when  $\phi \gg \phi_0$ ,<sup>16,18</sup> *i.e.*, in the supercritical region. However, as discussed in a recent *Perspective in Science*, “most reported power laws lack statistical support and mechanistic backing”.<sup>19</sup> The widely-used power law in CNP composites likely lies in the same situation. A sufficient statistical support for a candidate power law should exhibit a good linearity on a log-log plot over at least two orders of magnitude in both  $x$  and  $y$  axes.<sup>19</sup> Although some studies on CNP composites really provide such a statistical support for the observed power law,<sup>20,21</sup> the theoretical backing is still controversial. Usually, the *supercritical* power law, eqn (1), is correlated to the *critical* conductivity scaling law in classical percolation theory<sup>22</sup> which predicts that when  $\phi$  is above, but *very close* to, the percolation threshold  $\phi_c$ ,  $\sigma$  scales in a power law as

$$\sigma = \sigma_0(\phi - \phi_c)^t, \phi \rightarrow \phi_c^+, \quad (2)$$

where the critical conductivity exponent  $t$  is universal (system-independent) and only depends on dimensionality except for some special cases where long-range interactions are involved.<sup>23-26</sup> However, several factors make it dubious to identify eqn (1) as identical to eqn (2). First, it is clear in classical percolation theory<sup>22,27</sup> that eqn (2) applies only within the critical region  $\phi \rightarrow \phi_c^+$ , whereas eqn (1) is often valid even when  $\phi \gg \phi_c$ . Second,  $t$  in eqn (2) has universal values around 1.30 and 2.0 for 2D and 3D systems, respectively. But the experimentally extracted  $s$  from eqn (1) is strongly system-dependent.<sup>27</sup> A good example is that in the same (both 2D and 3D) systems comprising 1D conductive sticks (or fibers), simulations<sup>18,28</sup> have shown that  $s \approx 2$  for the junction-limit case (the resistance of junctions between two sticks  $R_j$  is much larger than the stick resistance  $R_s$ , i.e.,  $R_j \gg R_s$ ), while  $s \approx 1$  for the stick-limit case ( $R_s \gg R_j$ ). Last, it is very ambiguous<sup>29</sup> in most experimental studies whether the extracted  $\phi_0$  from eqn (1) coincides with the critical value  $\phi_c$  at the transition of structural connectedness which can be determined independently.<sup>30-32</sup> Through the same Monte Carlo simulations as in our early work,<sup>33</sup> we have studied systems comprising width-less conductive sticks (a simple model for carbon nanotubes or metal nanowires) and found that when the stick number density  $N$  ranges from 7 to 60 ( $N$  is much higher than the percolation threshold<sup>31</sup>  $N_c \approx 5.64$ ), eqn (1) gives perfect fitting to all the simulation data, but  $N_0$ , as well as  $s$ , significantly varies with the resistance ratio  $R_j/R_s$  and in general evidently deviates from the critical values, as shown in Fig. 1. As a matter of fact, once  $N_0$  is fixed to  $N_c$ ,  $s$  has to vary with  $N$ ,<sup>28</sup> that is to say, the power law is not valid any longer. Note that the deviation of  $N_0$  from  $N_c$  should not be ascribed to the non-nearest-neighbor tunneling<sup>29</sup> which is not considered in our simulations. Sometimes, the deviated  $s$  from  $t$  in Fig. 1c is regarded as the nonuniversal exponents.<sup>5, 23-26</sup> However, nonuniversality phenomena usually rely on certain junction resistance distribution<sup>23-26</sup> and should be identified within the critical region (close vicinity of percolation threshold).<sup>25-26</sup> On the one hand, our systems are all with constant junction

resistance. On the other hand, the stick systems has already been demonstrated as universal in the critical region.<sup>33</sup> Consequently, the deviated  $s$  in supercritical region is essentially different from the nonuniversality in critical region. All these suggest that eqn (1) is distinct from the critical conductivity scaling [eqn (2)]. As a result, eqn (1) lacks theoretical backing and its applicability is thereby not clear. More importantly, the vague meaning of  $\phi_0$  and the strongly system-dependent exponent  $s$  in eqn (1) prevent researchers from gaining any new insights into the conduction of CNP composites. Under these circumstances, we derive in this work a new scaling law for CNP composites.

It is challenging to unveil the true supercritical scaling within the framework of classical percolation theory which mainly focuses on the critical region. In contrast, effective medium theory (EMT) is extensively employed in disordered media in the supercritical region.<sup>34–37</sup> The main strategy of EMT is to determine the property (electrical conductivity, thermal conductivity, dielectric constant, etc.) of a composite system (e.g., CNPs embedded in an insulating matrix) through averaging the multiple values of the constituents (e.g., the CNPs and the surrounding matrix). However, the interactions between the inclusions (e.g., the inter-particle junctions) are often neglected.<sup>38</sup> This causes ineffectiveness of EMT for CNP composites where inter-particle junctions often dominate the system conductivity. Furthermore, clustering (aggregation) of CNPs is essential in all percolation systems, but is not considered in classical EMT either.<sup>9,37</sup> In this work, we propose a new concept, dynamic interfacial resistance (DIR), to overcome the drawbacks of EMT.

To involve the inter-particle junctions, in our model each particle is assumed to be *virtually* coated by a thin barrier layer, as illustrated in Fig. 2. The current flowing from one particle to another via the inter-particle junction is equivalent to that across the barrier layers. The barrier layer resistance, or the interfacial resistance, is inversely proportional to the

number of the junctions attaching to the particle (supposing all inter-particle junctions have identical resistance). As the average junction number increases with  $\phi$ , the interfacial resistance decreases with  $\phi$ , i.e., the interfacial resistance is dynamic. The advantages of the DIR model are three-fold. First, the physically existing inter-particle junctions are taken into account. Second, the effects of clustering have been partly addressed. Let us consider two typical cases. An isolated CNP (junction number is zero) has infinitely large interfacial resistance which rules out its contribution to the system conductivity. In contrast, CNPs standing in large clusters have big junction numbers and hence small interfacial resistance, enhancing their contribution to the system conductance. Last and most importantly, since the inter-particle junctions are replaced by the interfacial barrier layers, all the CNPs can be viewed as non-interacting and the classical EMT is still valid.

We consider a continuum percolation system consisting of ellipsoidal particles of conductivity  $\sigma_p$  embedded in a matrix of conductivity  $\sigma_m$  (usually  $\sigma_m \ll \sigma_p$ ). Ellipsoids represent a general shape for various CNPs. In different limiting cases, they may turn to be 1D fibers, sticks or rods, 2D flakes or disks, or 3D spheres.<sup>38,39</sup> All ellipsoidal particles are coated by a thin confocal resistive layer of thickness  $\delta$ . If a particle  $k$  has the junction number  $n_k$ , the resistance of its coating layer is  $R_{c,k} = R_j/n_k$  with  $R_j$  being the resistance of one junction.  $R_{c,k}$  may relate to the conductivity of the coating layer  $\sigma_s$  as  $R_{c,k} = \lim_{\sigma_s \rightarrow 0, \delta \rightarrow 0} \delta/\sigma_s$ .<sup>38,40</sup> The effective conductivity  $\sigma_k$  of such a coated ellipsoidal particle is<sup>38,40</sup>

$$\sigma_{k,i} = \frac{\sigma_p}{1 + L_i \sigma_p Q R_{c,k}} = \frac{\sigma_p}{1 + L_i \sigma_p Q R_j / n_k}, \quad i = x, y, z, \quad (3)$$

where  $\sigma_{k,i}$  is the component of  $\sigma_k$  aligned with the  $i$ th axis of the ellipsoid,  $L_i$  is the depolarization factor, and  $Q = a^{-1} + b^{-1} + c^{-1}$  with  $a$ ,  $b$ , and  $c$  being the ellipsoid radii. Impacted by the inter-particle junctions, the electric field distribution inside the particle  $k$  may alter. Hence  $L_i$  and  $Q$  in eqn (3) may deviate from the calculation based on the particle shape<sup>39</sup> and are denoted in this work as  $L_{k,i}^*$  and  $Q_k^*$ , respectively. Assuming the matrix particles have identical shape to the CNPs, one can obtain from the classical EMT<sup>41</sup> the effective conductivity  $\sigma$  of the percolation system as the solution of

$$\sum_k^{NV} \sum_i^{\Phi} \frac{L_{k,i}^*(\sigma - \sigma_{k,i})}{\sigma - L_{k,i}^*(\sigma - \sigma_{k,i})} + \sum_{k'}^{N'V} \sum_i^{\Phi} \frac{L_{k',i}^*(\sigma - \sigma_m)}{\sigma - L_{k',i}^*(\sigma - \sigma_m)} = 0, \quad (4)$$

where  $V$  is the system volume (or area in the 2D case where all CNPs lie in the  $x$ - $y$  plane),  $\Phi = \{x,y,z\}$  for 3D systems and  $\{x,y\}$  for 2D systems, and  $N$  and  $N'$  are the number density of the CNPs and matrix particles, respectively.

Most recent applications are interested in CNPs with the shape of sphere (e.g., silver/gold CNPs), laminated spheroid (e.g., graphene flakes) or fibrous spheroid (e.g., carbon nanotubes). For 3D systems, one may expect  $L_{k,x}^* \approx L_{k,y}^* \approx L_{k,z}^*$  for spheres;  $L_{k,x}^* \approx L_{k,y}^* \approx 0$  for laminated spheroids; and  $L_{k,z}^* \approx 0$  and  $L_{k,x}^* \approx L_{k,y}^*$  for fibrous spheroids. Therefore, for all these CNPs, eqn (4) approximates to the common form as

$$\sum_k^{NV} \frac{L_{k,i}^*(\sigma - \sigma_{k,i})}{\sigma - L_{k,i}^*(\sigma - \sigma_{k,i})} + \sum_{k'}^{N'V} \frac{L_{k',i}^*(\sigma - \sigma_m)}{\sigma - L_{k',i}^*(\sigma - \sigma_m)} = 0, \quad (5)$$

where  $i = x$  for spheres or fibrous spheroids, and  $i = z$  for laminated spheroids. For 2D systems, eqn (5) still holds with all  $i = x$ . For simplicity and generality, we suppose the supercritical percolation systems are highly uniform, so that eqn (5) can be simplified by directly replacing the particle ( $k$ )-dependent variables with their averages, that is

$$C \frac{X(\sigma - \bar{\sigma})}{\sigma - X(\sigma - \bar{\sigma})} + (1 - C) \frac{X(\sigma - \sigma_m)}{\sigma - X(\sigma - \sigma_m)} = 0, \quad (6)$$

where  $C$  is the volume fraction of the CNPs,  $X \equiv \langle L_{k,i}^* \rangle$ , and  $\bar{\sigma} \equiv \langle \sigma_{k,i} \rangle$ . According to eqn (3),

$$\bar{\sigma} \approx \frac{\sigma_p}{1 + X \sigma_p Q^* \langle n_k \rangle^{-1} R_j} \approx \frac{\sigma_p NV_{ex}}{NV_{ex} + X \sigma_p Q^* R_j} = \frac{\sigma_p C}{C + \beta X \sigma_p Q^* R_j}, \quad (7)$$

where  $Q^* \equiv \langle Q_k^* \rangle$  and since only the neighboring particles within the excluded volume (area)<sup>42</sup> can contact the particle  $k$ ,  $\langle n_k \rangle = (NV - 1)V_{ex}/V \approx NV_{ex} = C/\beta$  with  $V_{ex}$  being the excluded volume of a particle and  $\beta = C/NV_{ex}$  being a constant. Setting  $\sigma_m = 0$ , we obtain from eqns (6) and (7) that

$$\sigma = \frac{\sigma_p}{1 - X} \frac{C(C - X)}{C + \beta X \sigma_p Q^* R_j} = \sigma_0 \frac{\phi(\phi - \phi_0)}{\phi + M}, \quad (8)$$

where  $\phi = \alpha C$  with  $\alpha$  being a conversion factor,  $\phi_0 = \alpha X$ ,  $\sigma_0 = \sigma_p \alpha^{-1} (1 - X)^{-1}$ , and  $M = \alpha \beta X \sigma_p Q^* R_j \sim R_j / R_b$  with  $R_b$  being the bulk resistance of a CNP and  $\sigma_p Q^* \sim R_b^{-1}$  ( $R_b = R_s$  for the stick systems in Fig. 1). Because of the unpredictable deviation of depolarization factors induced by inter-particle interaction,  $X$  and thereby  $\phi_0$  is not known in our present theory. Nevertheless, eqn (8) has provided a new yet simple law for  $\sigma$  scaling as a function of  $\phi$ . In particular, since  $M \sim R_j / R_b$ , for junction-limit systems ( $R_j / R_b \gg 1$ ), one can expect  $M \gg \phi$ , and hence  $\sigma \approx \sigma_0 M^{-1} \phi(\phi - \phi_0) \sim \phi^2$ ; and for bulk-limit systems ( $R_j / R_b \ll 1$ ), one can expect  $M \ll \phi$ , and hence  $\sigma \approx \sigma_0 (\phi - \phi_0) \sim \phi$ . Straightforwardly, our new scaling law interprets the  $R_j / R_b$ -dependent exponents in various conductive fiber systems.<sup>18,28</sup> Moreover, it implies that the observed exponent  $s \approx 2$  in experiments should be ascribed to the dominance of junction resistance, not necessarily related to 3D systems whose  $t \approx 2$ . From our

theory, both 2D and 3D systems exhibit  $s \approx 2$  in junction-limit case. This has been verified by previous simulations.<sup>18</sup>

We revisit the 2D stick systems in Fig. 1 and find that eqn (8) provides fitting as excellent as eqn (1) (Figs. 1a and 1b). More importantly, the extracted  $N_0$  is much closer to the critical value  $N_c$  (Fig. 1d) especially when  $R_j/R_s > 1$ . Because the DIR model addresses partly the clustering effects, the approach of  $N_0$  to  $N_c$  is anticipated. However, when  $R_j \ll R_s$ , the impact of  $R_j$  in eqns (7) and (8) is almost negligible. Thereby, the DIR model is not effective to address the clustering effects in that case and the deviation of  $N_0$  from  $N_c$  is still evident. Fortunately, since most realistic systems of CNPs stay within the region  $R_j/R_s > 1$ , eqn (8) should apply extensively in practical systems. Once  $R_j/R_s \gg 1$  is confirmed, eqn (8) can be further reduced as

$$\sigma \approx \sigma'_0 \phi (\phi - \phi_0), \quad (9)$$

where  $\sigma'_0 \approx \sigma_0/M$ . That means only two parameters,  $\sigma'_0$  and  $\phi_0$ , are sufficient for the supercritical scaling. To verify this, we investigate electrical conductivity of three independent systems reported in the literature. They comprises carbon nanotubes,<sup>16</sup> graphene flakes<sup>15</sup> and spherical gold CNPs,<sup>9</sup> respectively. As shown in Fig. 3a, eqn (9) gives good fitting to all the systems, demonstrating its superiority to the power-law scaling [eqn (1)] which has to rely on three parameters with unclear physical meaning. In addition, we also study the thermal conductivity of junction-limited carbon nanotube networks<sup>43</sup> where the carbon nanotubes have different aspect ratios  $r = R_T/L_T$  with  $R_T$  being the tube radius and  $L_T$  the tube length. An analytical scaling law was derived<sup>43</sup> for the relative thermal conductivity as  $k_r = F(r)N^2$  with  $F(r) = 1/12\pi[1 + 8\pi r + (72 + 6\pi^2)r^2 + 96\pi r^3 + 24\pi^2 r^4]$ . This formula, however, only matches the asymptotic behavior of the numerical simulation results.<sup>43</sup> As shown in Fig. 3b, our eqn (9) gives excellent fitting to the simulation results throughout the

entire  $N$  region. Again, the extracted  $N_0$  ( $N_0 = 5.51$  for  $r = 0$  and  $N_0 = 4.04$  for  $r = 0.03$ ) agree well with their critical values ( $N_c \approx 5.64$  for  $r = 0$  and  $N_c \approx 4.88$  for  $r \approx 0.03$ ).<sup>31,32</sup> Furthermore, the extracted  $\sigma'_0$  ( $\sigma'_0 = 0.027$  for  $r = 0$  and  $\sigma'_0 = 0.050$  for  $r = 0.03$ ) is in excellent agreement with  $F(r)$  [ $F(0) = 1/12\pi \approx 0.0265$  and  $F(0.03) \approx 0.0499$ ]. These suggest that if the DIR model is considered in such systems, a more comprehensive scaling may be obtained simply as  $k_r = F(r)N(N - N_c)$ . Since in the junction-limited systems,  $\phi_0$  in our eqns (8) and (9) is close to the critical value  $\phi_c$ , this merit, in combination with the existing techniques or theory<sup>31,42</sup> for the determination of  $\phi_c$ , greatly enhances the predictive power of our scaling law.

However, it is worth noting that eqns (8) and (9) only apply to “genuine” percolation where only the junctions between two adjacent particles (or the nearest-neighbor tunneling)<sup>29</sup> contribute to the system conduction. Once tunneling between disconnecting CNPs (or high-order neighbors) dominates, the average interfacial resistance of the particles may scale as  $R_c \sim \phi^{-\alpha}$  ( $\alpha > 1$ ): In the case of tunneling, the junction resistance  $R_j$  drastically increases with the inter-particle distance  $d$ , which can be roughly expressed as  $R_j \sim d^\beta$  ( $\beta > 0$ ). With the increasing volume fraction  $\phi$ , the average distance  $d$  between the disconnecting CNPs decreases, that is  $d \sim \phi^{-\gamma}$  ( $\gamma > 0$ ), and hence  $R_j \sim \phi^{-\beta\gamma}$ . According to our DIR model,  $R_c \sim R_j / \phi \sim \phi^{-1-\beta\gamma} \equiv \phi^{-\alpha}$  with  $\alpha = 1 + \beta\gamma > 1$ . Then eqn (9) becomes  $\sigma_e \approx \sigma'_0 \phi^\alpha (\phi - \phi_0)$ . This may account for the higher-exponent power law [ $s > 2$  in eqn (1)] observed in some tunneling-dominated systems,<sup>5,27</sup> but has gone beyond the scope of the present work.

In summary, through the combination between the dynamic interfacial resistance model and the effective medium theory, this work derives a comprehensive yet simple scaling law for supercritical conductivity scaling of extensive pure percolation systems consisting of various conductive nanoparticles, including carbon nanotubes, graphene and spherical metal

nanoparticles. While the currently widely-used power law suffers from the lack of theoretical backing, our new scaling law is explanatory and predictive. We believe it will offer opportunities to gain genuinely new insights into a variety of practical applications based on conductive nanoparticles.

The simulations were performed on the computer clusters “Ferlin” and “Povel” at the PDC center in KTH. We acknowledge the financial support from the European Research Council through the Proof of Concept Grant (iPUBLIC, Grant No. 641416), the Swedish Research Council through the project grant iGRAPHENE (No. 2013-5759) and the framework grant (No. 2014-6160), and the Göran Gustafsson Foundation through the Young Research Prize (No. 1415 B).

1. E. S. Snow, J. P. Novak, P. M. Campbell and D. Park, *Appl. Phys. Lett.*, 2003, **82**, 2145–2147.
2. Q. Cao, H. Kim, N. Pimparkar, J. P. Kulkarni, C. Wang, M. Shim, K. Roy, M. A. Alam and J. A. Rogers, *Nature*, 2008, **454**, 495–500.
3. J. Li, T. Unander, A. López Cabezas, B. Shao, Z. Liu, Y. Feng, E. Bernales Forsberg, Z.-B. Zhang, I. Jögi, X. Gao, M. Boman, L.-R. Zheng, M. Östling, H.-E. Nilsson and S.-L. Zhang, *J. Appl. Phys.*, 2011, **109**, 084915.
4. C. K. Chan, H. Peng, G. Liu, K. McIlwrath, X. F. Zhang, R. A. Huggins and Y. Cui, *Nat. Nanotechnol.*, 2008, **3**, 31–35.
5. R. M. Mutiso and K. I. Winey, *Prog. Polym. Sci.*, 2015, **40**, 63-84.
6. J. N. Coleman, M. Lotya, A. O’Neill, S. D. Bergin, P. J. King, U. Khan, K. Young, A. Gaucher, S. De, R. J. Smith, I. V Shvets, S. K. Arora, G. Stanton, H.-Y. Kim, K. Lee, G. T. Kim, G. S. Duesberg, T. Hallam, J. J. Boland, J. J. Wang, J. F. Donegan, J. C. Grunlan, G. Moriarty, A. Shmeliov, R. J. Nicholls, J. M. Perkins, E. M. Grieveson, K. Theuwissen, D. W. McComb, P. D. Nellist and V. Nicolosi, *Science*, 2011, **331**, 568–571.
7. G. Pike and C. Seager, *Phys. Rev. B*, 1974, **10**, 1421–1434.

8. J. Li, M. M. Naiini, S. Vaziri, M. C. Lemme and M. Östling, *Adv. Funct. Mater.*, 2014, **24**, 6524–6531.
9. Y. Kim, J. Zhu, B. Yeom, M. Di Prima, X. Su, J.-G. Kim, S. J. Yoo, C. Uher and N. A. Kotov, *Nature*, 2013, **500**, 59–63.
10. J. Perelaer, B.-J. de Gans and U. S. Schubert, *Adv. Mater.*, 2006, **18**, 2101–2104.
11. J. Li, F. Ye, S. Vaziri, M. Muhammed, M. C. Lemme and M. Östling, *Adv. Mater.*, 2013, **25**, 3985–3992.
12. J. Li, M. C. Lemme and M. Ostling, *ChemPhysChem*, 2014, **15**, 3427–3434.
13. X. Huang, Z. Zeng, Z. Fan, J. Liu and H. Zhang, *Adv. Mater.*, 2012, **24**, 5976–6004.
14. H. Kim, A. a. Abdala and C. W. Macosko, *Macromolecules*, 2010, **43**, 6515–6530.
15. S. Stankovich, D. A. Dikin, G. H. B. Dommett, K. M. Kohlhaas, E. J. Zimney, E. A. Stach, R. D. Piner, S. T. Nguyen and R. S. Ruoff, *Nature*, 2006, **442**, 282–286.
16. F. M. Blighe, Y. R. Hernandez, W. J. Blau and J. N. Coleman, *Adv. Mater.*, 2007, **19**, 4443–4447.
17. L. Hu, D. Hecht and G. Grüner, *Nano Lett.*, 2004, **4**, 2513–2517.
18. P. Keblinski and F. Cleri, *Phys. Rev. B*, 2004, **69**, 184201.
19. M. P. H. Stumpf and M. A. Porter, *Science*, 2012, **335**, 665–666.
20. G. Cunningham, M. Lotya, N. McEvoy, G. S. Duesberg, P. van der Schoot and J. N. Coleman, *Nanoscale*, 2012, **4**, 6260–6264.
21. T. M. Higgins, D. McAteer, J. C. M. Coelho, B. M. Sanchez, Z. Gholamvand, G. Moriarty, N. McEvoy, N. C. Berner, G. S. Duesberg, V. Nicolosi and J. N. Coleman, *ACS Nano*, 2014, **8**, 9567-9579.
22. D. Stauffer and A. Aharony, *Introduction to Percolation Theory*, Taylor & Francis, London, 2nd revised edition, 2003.
23. I. Balberg, *Phys. Rev. Lett.*, 1987, **59**, 1305–1308.
24. C. Grimaldi and I. Balberg, *Phys. Rev. Lett.*, 2006, **96**, 066602.
25. P. M. Kogut and J. Straley, *J. Phys. C*, 1979, **12**, 2151-2159.
26. S. Feng, B. I. Halperin, and P. N. Sen, *Phys. Rev. B*, 1987, **35**, 197-214.

27. W. Bauhofer and J. Z. Kovacs, *Compos. Sci. Technol.*, 2009, **69**, 1486–1498.
28. M. Žeželj and I. Stanković, *Phys. Rev. B*, 2012, **86**, 134202.
29. D. Toker, D. Azulay, N. Shimoni, I. Balberg and O. Millo, *Phys. Rev. B*, 2003, **68**, 041403.
30. M. Newman and R. Ziff, *Phys. Rev. Lett.*, 2000, **85**, 4104–4107.
31. J. Li and S.-L. Zhang, *Phys. Rev. E*, 2009, **80**, 040104.
32. J. Li and M. Östling, *Phys. Rev. E*, 2013, **88**, 012101.
33. J. Li and S.-L. Zhang, *Phys. Rev. E*, 2010, **81**, 021120.
34. S. Kirkpatrick, *Phys. Rev. Lett.*, 1971, **27**, 1722–1725.
35. S. Kirkpatrick, *Rev. Mod. Phys.*, 1973, **45**, 574–588.
36. A. Davidson and M. Tinkham, *Phys. Rev. B*, 1976, **13**, 3261–3267.
37. C. G. Granqvist and O. Hunderi, *Phys. Rev. B*, 1978, **18**, 1554–1561.
38. C.-W. Nan, R. Birringer, D. R. Clarke and H. Gleiter, *J. Appl. Phys.*, 1997, **81**, 6692–6699.
39. S. Giordano, *J. Electrostat.*, 2003, **58**, 59–76.
40. X. F. Zhou and L. Gao, *J. Appl. Phys.*, 2006, **100**, 024913.
41. A. Davidson and M. Tinkham, *Phys. Rev. B*, 1976, **13**, 3261–3267.
42. I. Balberg, C. H. Anderson, A. S. and W. N., *Phys. Rev. B*, 1984, **30**, 3933–3943.
43. A. N. Volkov and L. V. Zhigilei, *Phys. Rev. Lett.*, 2010, **104**, 215902.

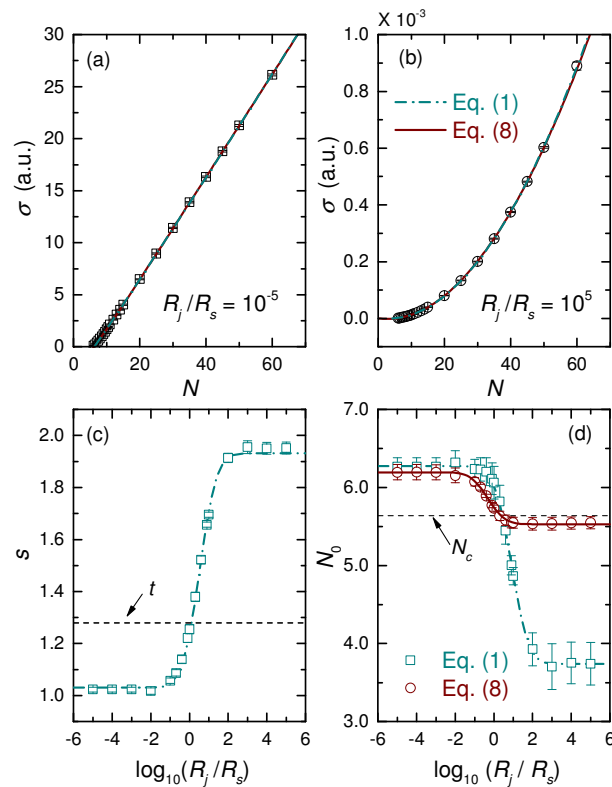


FIG 1. (color online) Monte Carlo simulation results for a 2D percolation system comprising width-less conductive sticks. All sticks have length  $l = 1$ , linear resistivity  $\rho = 1$ , and then resistance  $R_s = \rho l = 1$ . The system size is  $L = 30$ . (a,b) Simulated system conductivity  $\sigma$  (symbols) against  $N$  for (a)  $R_j/R_s = 10^{-5}$  and (b)  $R_j/R_s = 10^5$ . The curves are the data fittings by eqns (1) and (8). (c)  $s$  in eqn (1) and (d)  $N_0$  in eqns (1) and (8) extracted from the fittings to the simulated  $\sigma$  within  $7 \leq N \leq 60$  under different  $R_j/R_s$ . The curves are guides to the eyes.

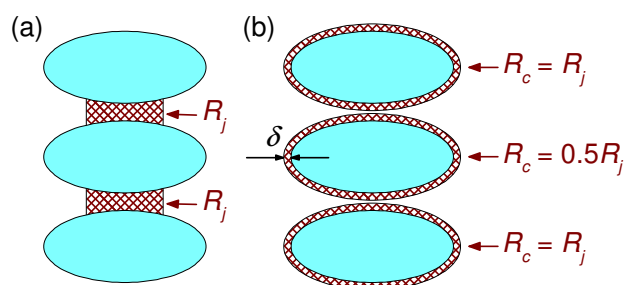


FIG 2. (color online) Illustration of the dynamical interfacial resistance model. (a) Three CNPs interacting through inter-particle junctions with resistance  $R_j$ . (b) The DIR model equivalent to (a). An inter-particle junction in (a) is replaced by thin barrier layers coating the two interacting CNPs, and hence the coated CNPs are viewed as non-interacting. For a coated CNP in (b), the interfacial resistance  $R_c$  is inversely proportional to its junction number in (a): The middle CNP has two junctions and  $R_c = R_j/2$ , while each of the others has one junction and  $R_c = R_j$ .

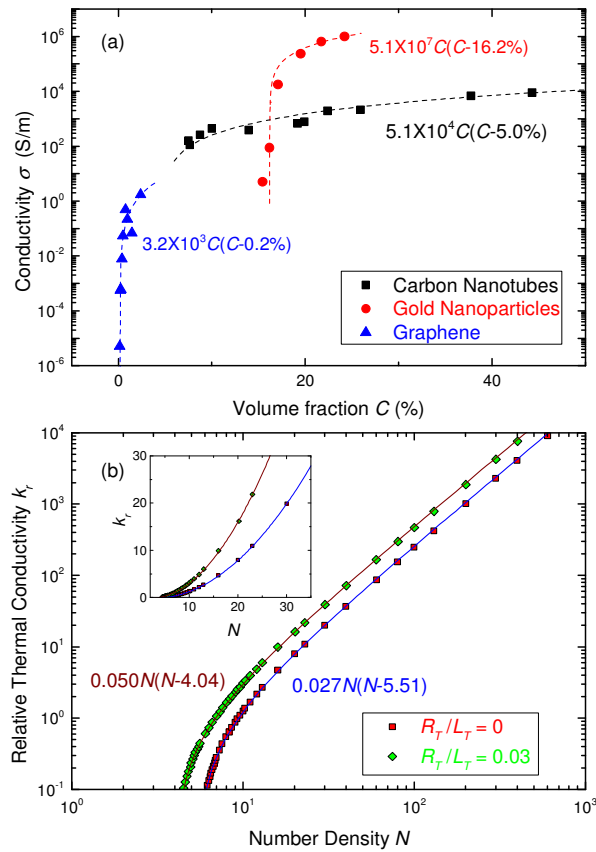


FIG 3. (color online) Data fittings of eqn (9) to (a) experimental electrical conductivity of percolation systems comprising different CNPs, and (b) numerically simulated thermal conductivity of carbon nanotube networks with different aspect ratios (for easy discussion, the nanotube length is set as  $L_T = 1$  in this work). All the curves are the fittings by eqn (9) with the fitted equations shown beside. In (a), the symbols for carbon nanotubes, graphene and spherical gold nanoparticles are experimental data from Fig. 4 in Ref. <sup>16</sup>, Fig. 3 in Ref. <sup>15</sup>, and Fig. 2 in Ref. <sup>9</sup>, respectively. In (b), the symbols are simulation data from Fig. 1 in Ref. <sup>43</sup>, and the inset is a close-up view of the low-density region.